ELSEVIER

Chemical Engineering Journal 91 (2003) 133–142

Chemical Engineering Journal

www.elsevier.com/locate/cej

New time-dependent Monte Carlo algorithm designed to model three-phase batch reactor processes: applications on 2,4-dinitro-toluene hydrogenation on Pd/C catalysts

Giampaolo Barone [a,b], Dario Duca [a,b,*]

[a] *Dipartimento di Chimica Inorganica ed Analitica, Università di Palermo, Viale delle Scienze, I-90128 Palermo, Italy*
[b] *Dipartimento di Scienze Farmaceutiche, Università di Salerno, Via Ponte don Melillo, I-84084 Fisciano, Salerno, Italy*

Abstract

The hydrogenation of 2,4-dinitro-toluene on a Pd/C catalyst was employed as a test reaction to simulate, by the time-dependent Monte Carlo method, processes occurring in a three-phase batch reactor working at isobar and isotherm conditions. A new time-dependent Monte Carlo algorithm, including an original subroutine useful to reduce the time of the simulations, was developed and implemented in Fortran language. The paper describes the flowchart of the code together with the main technical details and the involved physical and chemical models.

Computational characteristics, such as the simulated time to reach surface steady state conditions and the effects of the catalyst morphology are presented. Correlations between simulated and experimental data are summarized and current mechanistic hypotheses criticized.

Keywords: Three-phase batch reactor; Time-dependent Monte Carlo; Model in chemistry; 2,4-Dinitro-toluene hydrogenation

1. Introduction

The stochastic time-dependent Monte Carlo (tdMC) [1], method was used to test mechanistic hypotheses and understand laboratory data concerning catalytic reactions occurring in continuous flow bi-phase reactors [2–7]. This paper is to show how tdMC can successfully be employed to simulate heterogeneous catalytic reactions taking place in a three-phase batch reactor.

The 2,4-dinitro-toluene (2,4DNT) hydrogenation to 2,4-diamino-toluene (2,4DAT) on palladium/carbon, Pd/C, catalyst is here employed because on the whole the hydrogenation of di-nitro-aromatic compounds has relevant industrial applications [8–12] and, in particular, a significant example of this class of reactions is just represented by the 2,4DNT hydrogenation, being the 2,4DAT an important intermediate in the synthesis of toluene-di-isocyanate [12].

The title reaction was recently investigated in a three-phase batch reactor over Pd/C catalysts [13–18]. The complete, 2,4DNT → 2,4DAT, reaction occurred via a complex network. In the catalytic process, the experimentally non-distinguishable [17] 2-nitro-4-hydroxylamino-toluene and 2-hydroxylamino-4-nitro-toluene isomers (4HA2NT and 2HA4NT) and the separable 2-amino-4-nitro-toluene and 2-nitro-4-amino-toluene isomers (4A2NT and 2A4NT) were the isolated intermediates.

Taking into account these species, many different reaction mechanisms were hypothesized and tested [13,14] by employing traditional deterministic approaches to the description of the process dynamics, namely ordinary differential equation system (ODEs) approaches.

Experimentally, the distribution of the reaction products was affected by several factors including reaction temperature and catalyst morphology. Relating to the influence of the catalyst, it was suggested that the 2,4DNT hydrogenation could occur through a "structure sensitive" [14,18,19] mechanism. In details, it was hypothesized that the way of adsorption of the 2,4DNT species (see next section), affected by the palladium particle sizes, could be the determining factor in changing activity and selectivity of the catalyst [14]. On the whole, the title reaction was thoroughly investigated, both by experiments and ODEs method, reflecting the changes in the state of the adsorbed layer. Hence, to reproduce and/or explain the mechanistic features, arisen by these studies, is a good testing ground for the tdMC approach to the three-phase batch reactor catalytic processes.

* Corresponding author. Present address: Dipartimento di Chimica Inorganica ed Analitica, Università di Palermo, Viale delle Scienze, Parco d'Orleans II, I-90128 Palermo, Italy. Tel.: +39-091-489714; fax: +39-091-427584.
E-mail address: dduca@unipa.it (D. Duca).

1385-8947/02/$ – see front matter
PII: S1385-8947(02)00146-8

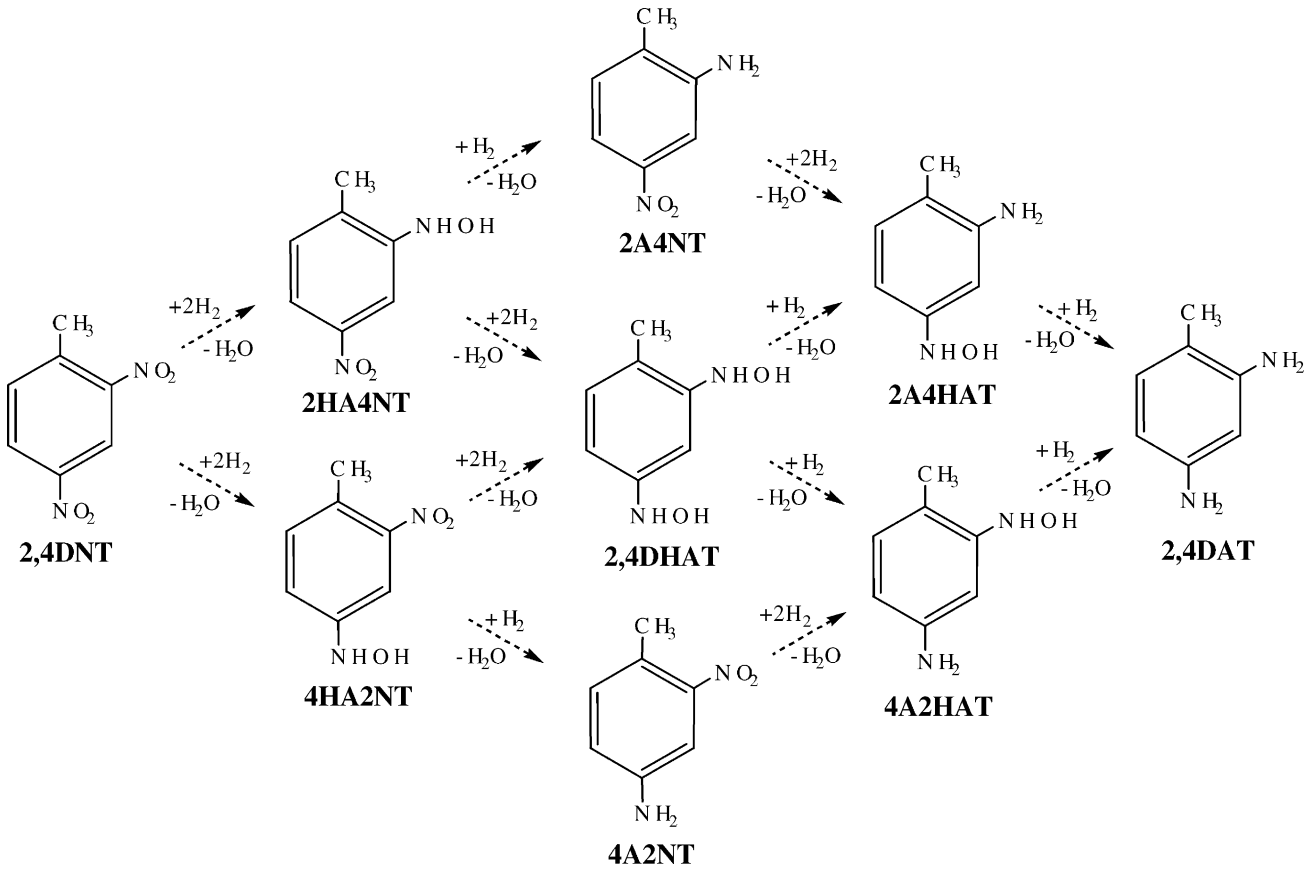

Scheme 1.

In fact, the tdMC technique lent itself easily for the representation of the catalyst surface population and composition during the reaction. Such a peculiarity proved to be effective in obtaining essential information on significant aspects of the catalytic hydrocarbon hydrogenation reactions [2–7] and in particular in rationalizing the structure sensitivity observed on different catalysts [5–7]. These findings, which were possible by mimicking the metal dispersion [5–7] and the steric hindrance of the surface species [2–7], were supported by ab initio quantum mechanical (QM) calculations, at HF and DFT levels [7,20].

Scheme 1 summarizes the hypothesized species and the reaction model used in the present work. No routes were set as the rate determining steps, whereas analogous species were considered to be involved both in solution and on the catalyst surface. The labels utilized for the molecule representations of Scheme 1 are also used to symbolize them in the text. The acronym HANT is employed to represent the, experimentally non-separable, pair 4HA2NT + 2HA4NT.

In the following section the tdMC algorithm with the physical and surface chemical models (Section 2.1) are presented together with the flow chart of the present home-made code (Section 2.2). The effects of the temperature, metal dispersion and reaction time on the activity–selectivity pattern of the title reaction and on the surface population and composition are shortly discussed in Section 3. These last aspects, however, are the extended subjects of two following papers, concerning with QM calculations and findings supporting the tdMC approach [21] and a new surface mechanism [22] proposed for the 2, 4DNT → 2, 4DAT reaction, rejecting the mechanistic hypotheses so far accepted [13–18].

2. The model

2.1. tdMC algorithm and details on chemical and physical models

In the tdMC approaches, the catalytic reaction is arranged into a set of elementary steps. To each of these steps an occurrence probability, P, is assigned [2–7] for given reference time and number of metal surface sites. These probabilities, whose sum during simulations is constrained to never exceed 1, are related to the activation energy, E_a, of the events [5–7,20] by the transition state theory. Due to this relation, the terms activation energy and occurrence probability can indifferently be employed for a given event. Reactive events, adsorption (hitting plus sticking) [20], desorption and diffusion phenomena are taken into account.

Owing to the intrinsic complexity of the present reaction system, we considered the reactive surface hydrogen atoms, i.e. the activated hydrogen on the metal-crystallite atop sites [4,5,20], like homogeneously distributed and sterically non-hindering surface species. The statements above imply a non-competitive hydrogen adsorption mechanism. This surface regime was already hypothesized [13] and is highly plausible because of the constant H_2 concentration found in solution [13,15]. Accordingly, we did not explicitly allow for events involving adsorption, diffusion and desorption of the H species, averaging their contributions into the whole process. Diffusion of toluene derivatives did not affect the simulation results. This is related to the sizes of the adsorption area on the metal crystallites of the toluene derivatives, which determines very low probabilities of surface traffic. Hence, after some preliminary simulations, the molecular surface diffusion was not considered.

Metal catalytic sites were reproduced by 100×100 squared matrices mimicking a mix of $\{1\,0\,0\}$ and $\{1\,1\,1\}$ fcc Pd faces. The simulation results did not change, irrespective of the relative amount between the sites present into the two different kinds of planes above. For the sake of simplicity, just the results relative to the $\{1\,0\,0\}$ fcc Pd system are here reported. Stationary boundary conditions and lateral interaction effects were also considered [4,5].

The species taken into consideration in the simulation were:

- in solution, 2,4DNT and 2,4DAT molecules and the seven possible intermediates (see Scheme 1);
- on the surface, for any of the solution molecules, the three different configurations exemplified for 2,4DNT in Fig. 1.

In this figure the dimensions of the spheres are normalized to the vdW radii of the atoms and the metallic sites labelled by x are considered as totally hindered, following the interaction probabilities of the surface species [7].

Because of the presence of the liquid phase, in the simulated experimental apparatus, we did not consider surface by-products, like polymer and/or carbonaceous deposits, supposing a continuous refreshing of the catalyst sites. The three different arrangements, we supposed to occur on the surface were:

- fat constellation, FC, in which the benzene plane of the adsorbed toluene derivatives is arranged in parallel way to the catalyst surface;
- hindered-flag and free-flag constellation, HFC and FFC, where the toluene derivatives interact with the Pd surface by a nitro or hydroxylamino or amino group in *ortho* or in *para* to the methyl fragment.

Before now, HFC surface species were not considered in the models employed to study the title reaction.

Ab initio QM calculations at HF level were performed on all the reagents, intermediates and products involved in the hydrogenation of 2,4DNT on Pd catalyst, to determine their structure, steric hindrance as well as other physical–chemical properties [21] relevant to the tdMC simulations.

The structures and the volumes of the species reported in Scheme 1, containing the light atoms H, C, N and O, were calculated by the extended split-valence double-zeta 6-31G(d,p) basis sets, with full optimization. The LANL2DZ pseudo-potential basis set [23] was employed to study model systems of species adsorbed on palladium surface. The calculations were performed using the GAUSSIAN98W package [24].

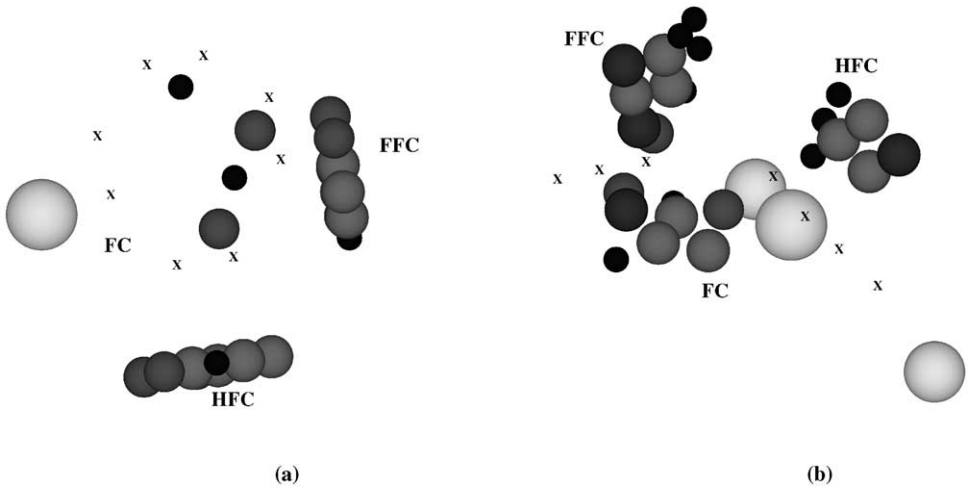

Fig. 1. 2,4DNT molecules adsorbed as FC, FFC and HFC on a $\{1\,0\,0\}$ plane of a Pd crystallite. The representations (a) and (b) show the same picture from different points of view. Pd atoms are represented by the light grey bigger spheres, the C atoms and the $-NO_2$ fragments by the dark grey medium sized spheres, the H atoms by the black smaller spheres.

Table 1
Species involved in the three-phase 2,4-dinitro-toluene hydrogenation and their calculated volumes in solution

Species[a]	Volume (nm^3)	R (nm)[b]
2,4DNT	0.38	0.45
4HA2NT	0.38	0.45
2HA4NT	0.33	0.43
4A2NT	0.33	0.43
2A4NT	0.38	0.45
2,4DHAT	0.36	0.44
4A2HAT	0.33	0.43
2A4HAT	0.33	0.43
2,4DAT	0.29	0.41
H_2O	0.07	0.25

[a] For the meaning of the labels, see Scheme 1. Hydrogen, which is not explicitly included in the simulations (see text), is not considered in this table.
[b] Radius of gyration of the species, assumed as spherically shaped [25].

Here, the essential information is given about the QM findings. By means of these calculations we could:

- evaluate the volume occupied by the species in solution (see Table 1);
- visualize the interaction modes of the species with the catalyst surface;
- determine the number of hindered sites (12 and 4 and 3 for FC and HFC and FFC), see Fig. 1;
- obtain a qualitative desorption activation energy order of the different species on the Pd surface.

Knowing the volume of the species in the ethanol solution we could determine, by the diffusion-limited rate constant theory [26], the hitting probability of the solvated species. The hitting of water was used to monitor the elapsing time, hence to set the internal clock, which allowed us [2–5] the kinetic study. The production of water occurring along with the reaction did not affect the timing procedure. Sticking probability of the toluene derivatives on free surface was set equal to 1 [27]. Formation of multi-layers of adsorbed species was not allowed. Although the program could also account of the water and ethanol sticking and of the surface deposit formation, we did not explicitly consider these events.

In order to reduce the number of parameters to be considered, the desorption probabilities of the different FC toluene species were usually set constant, irrespective of the substituting fragments present in the molecule. The desorption probability of HFC and FFC species adsorbed through equivalent fragments were also considered equal. Both these positions can be easily justified, considering a stronger adsorption interaction contribute due to the aromatic ring fragment with respect to the nitro or hydroxylamino groups and the well-known analogous reactive behaviour of the *ortho* and *para* substituting fragments. The probability of reaction of the $–NO_2$ and the –NHOH fragments, hence the corresponding E_a, were also non-dependent on the considered FC, HFC and FFC toluene derivatives. The admissibility to reduce the number of parameters was confirmed by preliminary simulations performed using larger sets of parameters. These simulations showed a non-significant improvement in reproducing experimental details.

This standpoint is supported, at least for the occurrence probabilities of the $–NO_2$ fragment hydrogenation, by the data published by Neri et al. [13]. In fact, considering the reported rate constants at 323 K for the hydrogenation of *ortho* and *para* $–NO_2$ groups in different toluene derivatives [13], by the transition state theory [4,5], we can estimate a difference in the activation energy of the $–NO_2$ reactivity events in the ranges 2.6–4.7 and 0.5–1.6 kJ mol^{-1} for different positions in the same derivative and the same position in different derivatives, respectively.

Although we imposed a quite limited number of parameters, this tdMC code is able to take into account almost all the constraints (such as the influence of the methyl group on the desorption or reaction process of a given fragment), which could be thought for modelling the title reaction.

The physical characteristics of the catalytic system could be mimicked by normalizing, to the number of the matrix sites, the values of the experimental extensive variables and leaving unchanged that of the intensive ones, knowing the total experimental exposed metal surface area and solution volume. Actually, as represented in Fig. 2, from the whole solution, which is in contact with the gas phase, we isolated micro-portions (effectively simulated system) constituted by a metal particle of 10 000 sites centred in a drop of solution.

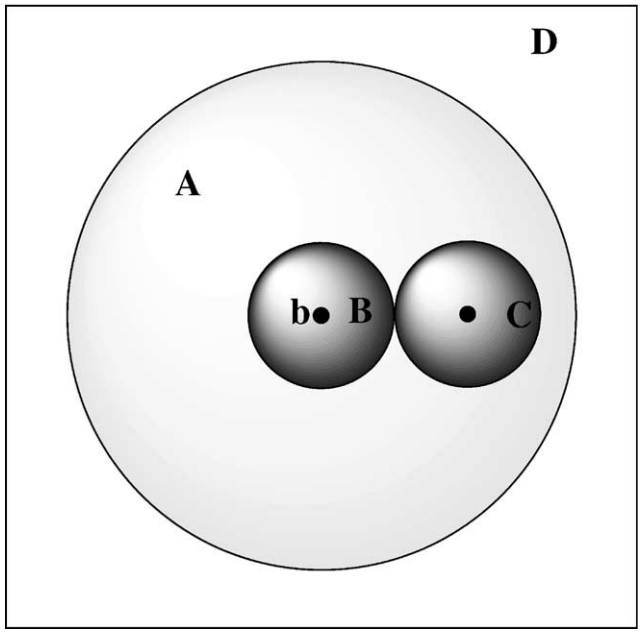

Fig. 2. Three-phase batch reactor model; solution phase: sphere A; gas phase: environment D; system micro-portion: sphere B or C. System micro-portion is constituted by a metal particle, sphere b, centred in a solution drop. The volume of this is normalized to the area of the simulated metallic sites, knowing the experimental exposed metal surface area and solution volume.

It has to be noticed that in the model of Fig. 2, radii of the spherical regions are not scaled down whereas the metal surfaces are spherical, due to the periodic-boundary conditions imposed. To model the experimental metal dispersion, D_x, of the metal catalyst, an adequate number of surface gaps [5], 0–50% of the total surface sites, was introduced on the surface matrix before starting the simulations. The model assumes chemical regime conditions, which effectively were verified during the experiments [16]. Besides the H_2 concentration, fixed in solution, the chemical characteristics of this, and of course of the surface phase changed dynamically along the reaction while its temperature was maintained constant.

The analysis and description of less common peculiarities, characteristics and feasibilities, of the here presented tdMC algorithm are the subjects of next papers [21,22].

2.2. Flow chart of the code and technical details

Scheme 2 presented the flow diagram of the home-made tdMC algorithm, implemented in standard Fortran as KÖVÉR.FOR. The sub-units containing the acronym (rn) used RAN2, a portable random number generator described in "Numerical Recipes" [28].

In the INPUT box the temperature, the H_2 pressure, the volume and the total concentration of the solution are defined together with the number, kind and starting molar ratio of the species involved in the reaction system. In the same context the total time of the simulation (simulated time), the activation energies, useful to define the event occurrence probabilities, the metal dispersion and the volumes and the sites occupied by the species in solution and on the surface are fixed. At the end of the simulation, the mimicked activity–selectivity results, taken at different simulation times, are sent to the OUTPUT box. Here, the results above, mainly related to species disappeared from or produced inside the solution, are compared with the experimental ones in order to validate the starting set of E_a parameters used in the simulation.

The E_a values were fixed considering experimental results [13,15] and related preliminary QM findings [21], "ceiling" E_a parameter values. However, enclosing KÖVÉR in a minimization procedure [22], namely AMOEBA of "Numerical Recipes" [28], in which experimental activity–selectivity data [14,18] were fitted, we could refine the ceiling E_a values so as to obtain more confident parameters, "fitting" E_a parameters.

Subroutines attiva and proba, at the beginning of the program run, calculate, by the INPUT information, the maximum occurrence probability values of the events on clean surface (see Footnote a of Table 3) and state the optimized time unit (about 10^{-10}–10^{-11} s), regular time of Scheme 2.

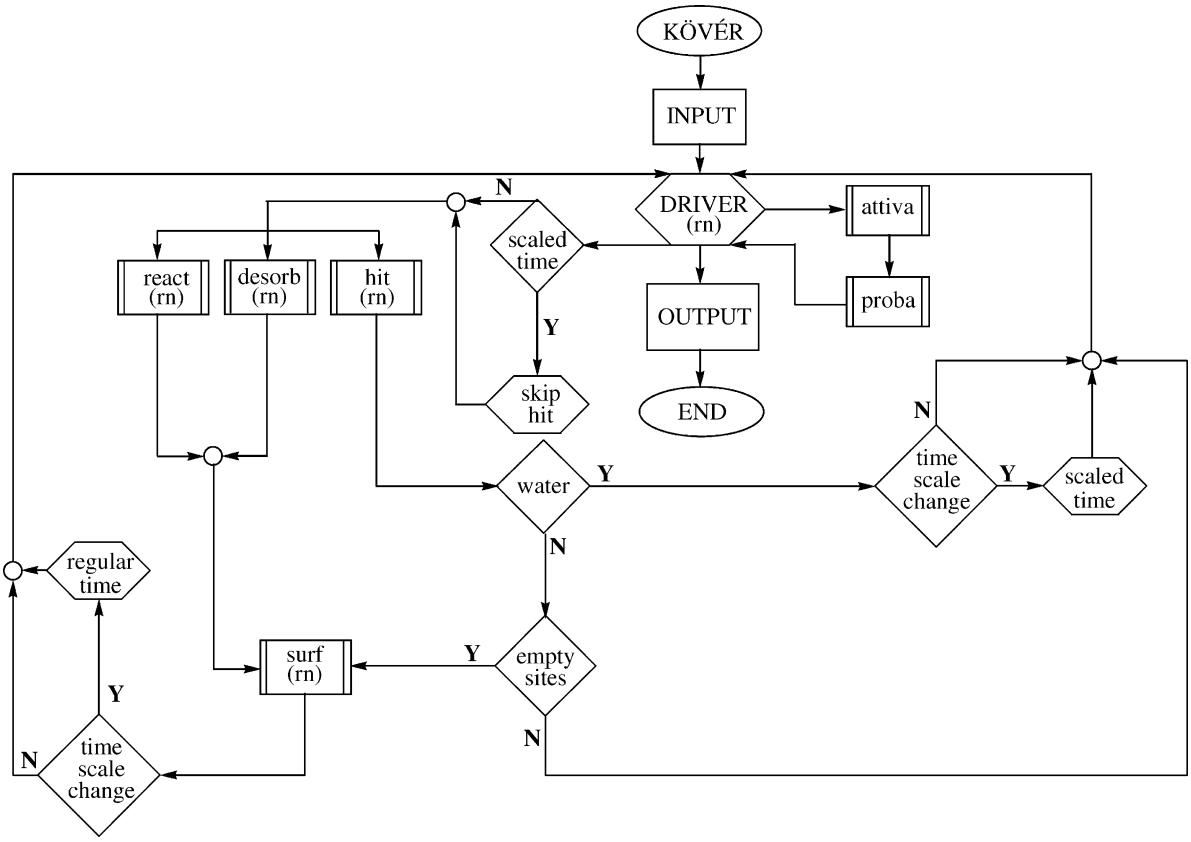

Scheme 2.

This is the larger time value able to constrain the event occurrence probability sum, until the end of simulation, into the unitary digit. Knowing the details on the surface population and the actual time unit, the sub-unity DRIVER randomly chooses one event (the null event also included) from a comb of possibilities. Subroutines react, desorb and hit handle these passages, respectively, for reaction, desorption and hitting-adsorption events. If one of these events has occurred, subroutine surf determines in which position of the mimicked surface it has happened and records the new surface population.

Subroutines react and desorb are called just for species already present on the surface. Hence, as shown in Scheme 2, the surface population is modified every time they are called. On the contrary, the hit of a given derivative leads to surface changes only if: (a) the hitting is not of a water molecule (box, *water*) and (b) some room is present on the same surface (box, *empty sites*).

Timing procedure, in the present tdMC code, shows a new routine (the cluster of sub-units, scaled time plus regular time), which allows the algorithm to change the sizes of the time unit, from regular to scaled time (box time scale change followed by the sub-unit scaled time), when, due to the surface constellations reached, the occurring events become only the hitting of solvent or of solvated molecules. In this case (the option is switched on after a given number of consecutive non-adsorbing hitting events occurred), the hitting events are momentarily skipped from the comb of the possibilities and the choice is done among the remaining surface events. Following the occurrence of one of these events, the simulated time is incremented as the inverse of its occurrence frequency (i.e. probability) value, normalized to the size of the mimicked surface. After this chronological jump, which ranges between values about one-order of magnitude larger than the unit time and 1% of the total simulated time, the time calculation procedure is restored from scaled to regular time (box time scale change followed by sub-unit regular time). By this procedure, no information is lost while the simulation time is shortened of several magnitude orders and the simulated reaction time easily reaches values comparable to the real reaction time.

After the occurrence of any events the line returns to DRIVER, which monitors the elapsed simulation time and stops the code when the total time, time to be simulated, is reached.

Simulations were performed on different platforms, usually IBM-PC Pentium II-IV working with 300–1400 MHz processors, under LINUX and W98 environments. Simulations were stopped at the surface system pseudo-steady-state conditions. This condition is reached when the surface population values of the main involved species, occupying at least 1% of the surface sites, show, in the final 30% of the total simulated time, an average deviation from the media no larger than 10%. To reach the surface pseudo-steady-state, simulated reaction time of 0.1–10 s were usually sufficient. A single calculation, that is a simulation at arbitrary time of given experimental conditions, lasted 1–30 min on a PC-PIII 600 MHz, depending on the amount of the species involved in the simulation. Reaction times of few minutes were even modelled whereas vivid pictorial images of the surface populations were obtained by Visual Fortran codification.

3. Results and discussion

The mimicked experimental results concern the 2,4DNT hydrogenation occurred on a Pd/C catalyst, MGPd5 in Ref. [14]. The catalyst was studied by XRD, TEM and CO chemisorption. The CO/Pd ratio was equal to 0.27, whereas the metal particle size resulted 4.1 and 4.0 nm by CO chemisorption and TEM, respectively. The reaction was carried out in ethanol medium (starting concentration of 2,4DNT equal to 0.1 M) at constant pressure of H_2, 1 atm, in a three-phase batch reactor at 323.15 K. The progress of the reaction was followed by gas- and liquid-chromatography.

The experimental appearance–disappearance ($r\pm$) rates, in the solution phase, per surface metal site per second of the 2,4DNT, HANT, 4A2NT, 2A4NT and 2,4DAT species, at different reaction times, were reproduced in a fit, to refine the values of the ceiling parameters [22]. The times at which we considered the $r\pm$ values of the five species were 10, homogeneously distributed from 0 to 180 min. The 5×10 simulated points were taken at surface pseudo-steady-state conditions. The comparison between experimental [14] and simulated data is reported in Table 2. Details on the fitting results are given in Ref. [22].

The refined physical–chemical reaction parameters [22] are reported in Table 3. Of course, only averaged E_a values, involving the same fragments and actions, could be obtained considering the events described in Section 2.1. In order to test the reliability of the refined parameters of Table 3 and the flexibility of the tdMC algorithm, in the following we illustrate the outcomes on the surface population and the corresponding macroscopic effects due to the changes on metal dispersion, reaction time and temperature, which were not explicitly considered in the fit process. If not explicitly indicated, the simulated conditions are those reported at the beginning of this section. The findings summarized in Tables 4 and 5 and the surface populations illustrated by Figs. 4 and 5 were obtained at the starting reaction time, $t = 0$ min.

Table 4 clearly demonstrates that the catalytic activity decreases as the metal dispersion increases. Table 5 shows that, increasing the metal dispersion, the selectivity to HANT decreases, whereas that to 4A2NT increases and to 2A4NT is almost constant. The behaviours described in Tables 4 and 5 are in well agreement with the experimental ones [14,18]. Hence we are confident on the refined parameters of Table 3. The trend of the parameter values of the last column in Tables 4 and 5 allows one to explain the experimental findings. In fact, since the surface 2,4DNT fat species are almost absent [22], the change in activity can be attributed to the decreasing of the whole amount of flag

Table 2
Experimental and simulated appearance–disappearance rates (per surface metal site per second), $r\pm$, at different times

Time (s)	$10^2 \times r\pm$(2,4DNT[a]/s^{-1})	$10^2 \times r\pm$(HANT[a]/s^{-1})	$10^2 \times r\pm$(4A2NT[a]/s^{-1})	$10^2 \times r\pm$(2A4NT[a]/s^{-1})	$10^2 \times (r\pm$2,4DAT[a]/s^{-1})
0.00×10^0	−42.0/−42.0	+19.7/+13.0	+3.28/+1.70	+1.31/+0.25	0.00/0.00
1.20×10^3	−42.0/−38.9	+19.7/+18.2	+3.28/+3.20	+0.66/+0.10	0.00/0.00
2.40×10^3	0.00/0.00	−5.91/−12.0	+1.97/+3.80	+0.66/+0.10	+1.31/+0.20
3.60×10^3	0.00/0.00	−5.91/−10.2	+1.31/+1.50	0.00/0.00	+3.94/+0.40
4.80×10^3	0.00/0.00	−5.91/−8.20	+0.66/+1.30	0.00/−0.93	+3.94/+0.80
6.00×10^3	0.00/0.00	−5.91/−7.32	0.00/0.00	+0.66/−2.00	+6.57/+1.60
7.20×10^3	0.00/0.00	−4.60/−5.04	−1.97/−0.80	−0.66/−3.00	+6.57/+2.50
8.40×10^3	0.00/0.00	−4.60/−2.00	−1.97/−1.00	−0.66/−3.00	+6.57/+3.00
9.60×10^3	0.00/0.00	−1.97/−1.88	−1.97/−2.00	0.00/0.00	+6.57/+4.00
1.08×10^4	0.00/0.00	0.00/0.00	−1.97/−2.00	0.00/0.00	+6.57/+5.00

[a] Experimental/simulated appearance–disappearance rate values per surface metal site per second. Experimental data are obtained from Ref. [14]. In table, (+) and (−) symbols are representing appearance and disappearance, respectively. Simulations were performed employing the physical–chemical parameters of Table 3.

2,4DNT surface species, $\theta_{(FFC+HFC)}$ values. Conversely, the selectivity pattern can be accounted for by the changes, with D_x, observed in both $\theta_{(FFC+HFC)}$ and $\theta_{FFC}/\theta_{HFC}$ parameters. In fact, the behaviour of the former suggests a relative increment of the surface amount of the hydroxylamine with respect to the nitro species as the metal dispersion increases, if the hydrogenation rate of a single nitro group remains constant. The behaviour of the second parameter shows an increase of the *para* adsorbed species with respect to the *ortho*. Therefore, the first behaviour explains the decrease of the selectivity to HANT molecules (second column of Table 5), the second the increase of the selectivity to 4A2NT with respect to the selectivity to 2A4NT (third and fourth columns of Table 5), occurring with the increase of D_x.

Fig. 3 shows the surface population and composition at $t = 0$ min (total concentration 0.1 M; starting 2,4DNT molar ratio 1) and $t = 180$ min (total concentration 0.1 M; starting 4A2NT and 2,4DAT molar ratios 0.04 and 0.96, respectively). Even in the latter, the simulation was initiated on a fresh catalyst surface. This is because, considering the

Table 3
Averaged event occurrence probabilities on surface (per whole surface sites, per ps at 323.15 K) normalized to the number of the sites occupied by the different surface species configurations, and corresponding activation energy values for the different event considered in the title reaction

Event	P[a]	E_a (kJ mol^{-1})[b]
r-NO_2[c]	$7.8(8) \times 10^{-13}$	79(5)
r-NHOH[c]	$2.4(1) \times 10^{-12}$	76(3)
d-NO_2[d]	$1.1(4) \times 10^{-12}$	79(2)
d-NHOH[d]	$1.0(7) \times 10^{-11}$	73(6)
d-NH_2[d]	$1.0(9) \times 10^{-6}$	42(3)
d-Φ[e]	$1.1(4) \times 10^{-12}$	79(4)

[a] Determined employing the transition state theory [4,5], by the E_a values. Note that adsorption of the studied species actually occurs on 12 (FC), 4 (HFC) and 3 (FFC) surface sites; hence homonym event occurrence probabilities on the same catalytic surface change along with the different configurations. In detail, the probabilities reported in this table are those of hypothetical surface species adsorbed on one site of unoccupied surface (maximum probabilities). To obtain the probabilities for FC, HFC and FFC the corresponding values have to be divided for the number of the surface sites, occupied in the different configurations.
[b] E_a values are refined by the fit procedure. Details on this procedure are given in Ref. [22].
[c] r-X is the averaged, with respect to different fat and flag molecular configurations, surface reactivity of the fragment X.
[d] d-X represents the averaged, with respect to different flag molecular configurations, desorption ability of the fragment X.
[e] Averaged desorption probability of the different fat molecules on the metal surface.

Table 4
Simulated catalyst relative activity (c.r.a.) at $t = 0$ min, in the 2,4DNT hydrogenation and corresponding surface molar ratio sum of the 2,4DNT-HFC and -FFC species, $\theta_{(FFC+HFC)}$, on Pd/C catalyst, at different D_x

D_x	c.r.a.[a]	$\theta_{(FFC+HFC)}$[b]
0.0	1.00	0.77
0.3	0.77	0.71
0.6	0.60	0.65
0.9	0.50	0.49

[a] c.r.a. is defined as the activity of a catalyst, with a given D_x, normalized to the activity of a reference catalyst, having D_x equal to 0.
[b] The surface molar ratio θ_x is the ratio between the number of surface sites occupied and/or hindered by the species x and the total number of available surface sites; $\theta_{(FFC+HFC)}$ is the sum of FFC and HFC surface molar ratios for 2,4DNT species. Fat species are almost absent at $t = 0$ min [21,22].

Table 5
Simulated selectivity, at $t = 0$ min, to HANT, 4A2NT and 2A4NT occurring with 2,4DNT hydrogenation on Pd catalysts at different D_x and relative amount of the FFC and HFC surface molar ratios of 2,4DNT species, $\theta_{FFC}/\theta_{HFC}$

D_x	S_{HANT}[a]	S_{4A2NT}[a]	S_{2A4NT}[a]	$\theta_{FFC}/\theta_{HFC}$
0.0	0.96	0.03	0.01	3.7
0.3	0.92	0.06	0.02	4.5
0.6	0.87	0.12	0.01	5.1
0.9	0.80	0.18	0.02	5.7

[a] The selectivity, S_x, to a certain product x, determined in the solution phase, is the ratio between the number of product species and the total number of molecules produced, at a given time of the reaction.

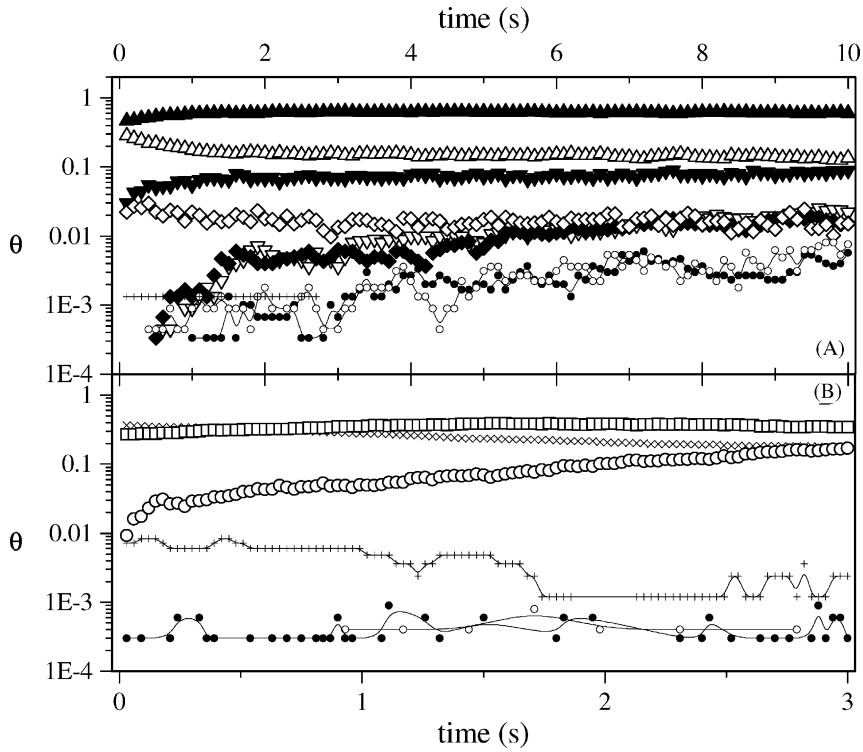

Fig. 3. Surface population occurring with the hydrogenation of 2,4DNT on Pd catalysts at different simulation times. Cross symbols represent FC species, solid and open symbols FFC and HFC species. (A) $t = 0$ min, 2,4DNT (up-triangle), 4HA2NT (down-triangle), 2HA4NT (diamond). (B) $t = 180$ min, 2HA4AT (circle), 2N4AT (square), FC-2,4DAT (×). Flag and fat noising species, see text, are represented in (A) and (B) as (small circle) and (+).

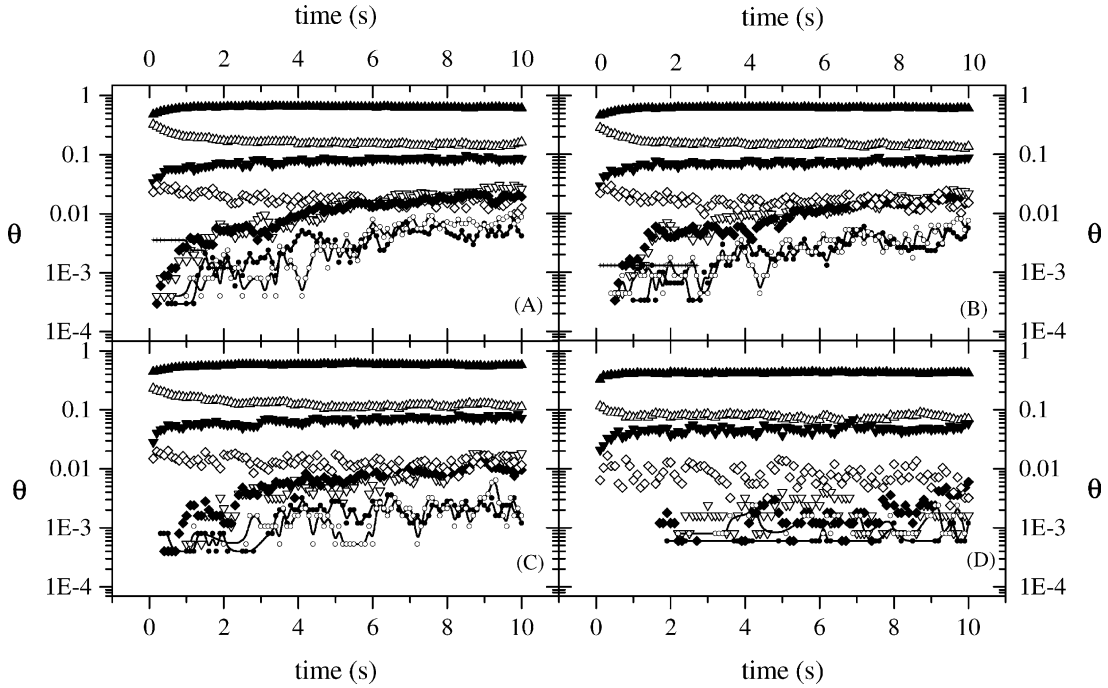

Fig. 4. Surface population found during the hydrogenation of 2,4DNT on catalysts at different D_x. In (A), (B), (C), and (D), D_x values are 0.0, 0.3, 0.6 and 0.9. Cross and solid and open symbols represent FC and FFC and HFC species: 2,4DNT (up-triangle), 4HA2NT (down-triangle), 2HA4NT (diamond), flag noising species (small circle), fat noising species (+).

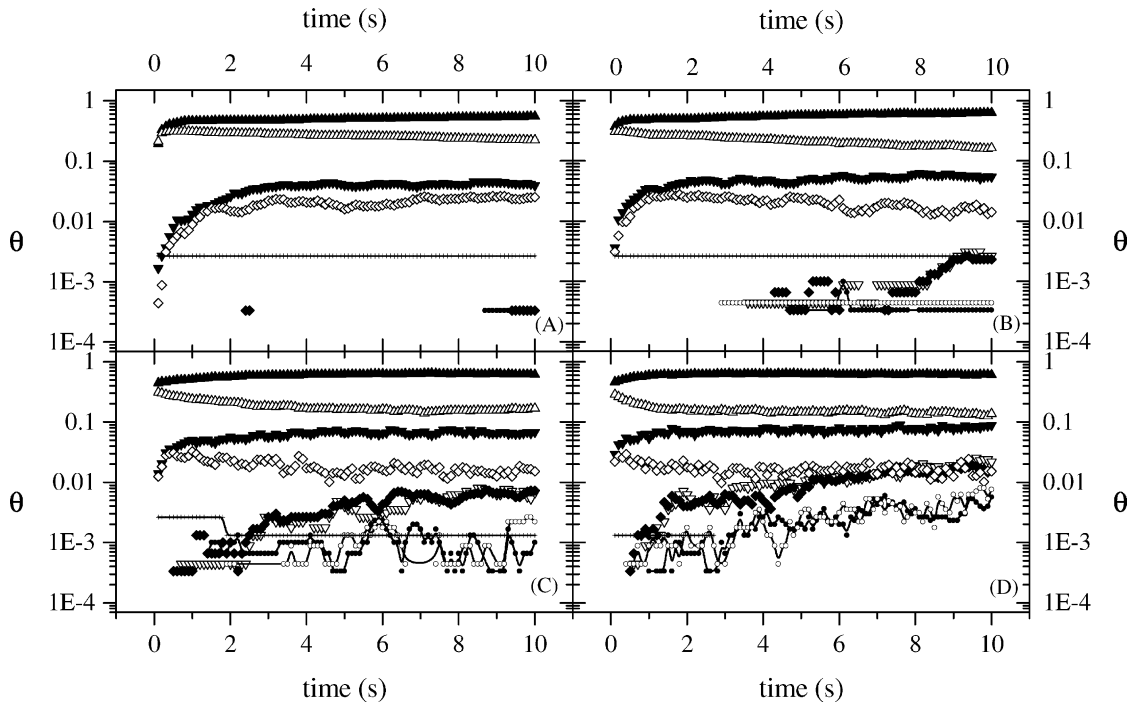

Fig. 5. Surface population found during the hydrogenation of 2,4DNT on a catalyst at different temperatures: in (A), (B), (C), and (D), temperature values are 293.15, 303.15, 313.15 and 323.15 K. Cross, solid and open symbols represent FC, FFC and HFC species, respectively; 2,4DNT (up-triangle), 4HA2NT (down-triangle), 2HA4NT (diamond), flag noising species (small circle), fat noising species (cross).

solution species experimentally isolated [13–16] at a given time and assuming a fast exchange between solution and surface molecules, at mimicked surface pseudo-steady-state conditions we are confident to be very close to the true surface population. In Figs. 3–5, fat and flag noising species are represented. The surface noising species have surface coverage values always below 1% of the total catalyst surface, whereas the surface molar ratio of noising species, e.g. fat noising species, is the sum of the surface molar ratios of all the noising species that have analogous surface constellation, e.g. FC.

Fig. 3 A and B show that, at different reaction times, the surface population and composition change dramatically. In particular, different surface regimes occur on the surface: a flag regime (picture A), where at the beginning of the reaction FFC and HFC species are mainly present, and a fat regime that characterizes the end of the process, in which 2,4DAT-FC species predominate [22] (picture B). Of course, during the reaction, intermediate situations characterize the catalyst surface whilst, correspondingly, the macroscopic activity–selectivity pattern dynamically changes.

Figs. 4 and 5 show the surface effects occurring with the changes of the metal dispersion and temperature. The surface population and composition of Fig. 4 help to understand the activity–selectivity pattern summarized in Tables 4 and 5 [22]. Fig. 5, which reports at different temperatures the surface characteristics of a catalyst at the starting reaction time, shows that the reaction temperatures significantly affect the relative amounts of the surface species. This could certainly have consequences on the Arrhenius analysis of this system and more generally of reaction systems involving surface processes [21,22].

With the three last figures we wanted just to show the ability of our model to mimic different experimental situations and incidentally we pointed out some consequential implications. These, which are extensively discussed in Refs. [21,22], are summarized in the following.

Our approach allowed us to:

- link QM energetic findings to tdMC kinetic results;
- state that, besides the already considered FFC and FC surface toluene derivatives [14], HFC species play an important role in the surface mechanism.
- relate the microscopic surface species and actions to the macroscopic activity–selectivity pattern;
- mimic surface processes non-experimentally tested, e.g. adsorption–desorption of toluene derivatives non-involving hydrogenation;
- reproduce the experimental activation energy of the whole 2,4DNT hydrogenation;
- interpret the role of the steric hindrance and of the metal dispersion on the reaction mechanism;
- criticize the so far accepted mechanistic interpretation [13–15,18] and propose a new reaction mechanism.

As regards the last point, many surface reaction hypotheses, like that suggesting hydrogenation steps as occurring

on two sites [15], one occupied by hydrogen and one by the species to be hydrogenated, proved to be non-physical by the present tdMC approach [22].

4. Conclusion

This study, by the example of the 2,4DNT hydrogenation on Pd/C catalysts, shows that tdMC models can be employed to simulate three-phase batch reactor processes. A large number of different species and their actions, occurring into several phases at different reaction conditions, could be easily handled with fairly small use of computing time also on common PCs working, by Fortran codes, under different operative systems.

Quantum mechanical calculations help to get starting information on basis phenomena to be considered in the simulations. This, together with the consideration of experimental data, can lead to determine ceiling values of the event occurrence probabilities whereas a successive refining fit procedure allows one to reach more realistic results.

In short, this method showed to be able:

- to reproduce the inmost physical and chemical characteristics using a concise representation of the title reaction events,
- to point the role of the species, even of those ones experimentally not isolated,
- to predict aspects not yet investigated.

Acknowledgements

Authors thank Professor Giovanni Neri, Department of Industrial Chemistry, University of Messina, for having suggested this study and for the very helpful and clarifying discussions.

References

[1] B.J. Garrison, P.B.S. Kodali, D. Srivastava, Chem. Rev. 96 (1996) 1327. and references therein.
[2] D. Duca, L. Botár, T. Vidóczy, J. Catal. 162 (1996) 260.
[3] D. Duca, P. Baranyai, T. Vidóczy, J. Comp. Chem. 19 (1998) 396.
[4] D. Duca, G. La Manna, M.R. Russo, Phys. Chem. Chem. Phys. 1 (1999) 1375.
[5] D. Duca, G. La Manna, Zs. Varga, T. Vidóczy, Theoret. Chem. Acc. 104 (2000) 302.
[6] D. Duca, G. Barone, Zs. Varga, Catal. Lett. 72 (2001) 17.
[7] D. Duca, G. Barone, Zs. Varga, G. La Manna, J. Mol. Struct. (Theochem) 542 (2001) 207.
[8] O.M. Kut, F. Yuculen, G. Gut, J. Chem. Technol. Biotechnol. 39 (1987) 107. and references therein.
[9] H.J. Janssen, A.J. Kruithof, G.J. Steghuis, K.R. Westerterp, Ind. Eng. Chem. Res. 29 (1990) 754.
[10] H.J. Janssen, A.J. Kruithof, G.J. Steghuis, K.R. Westerterp, Ind. Eng. Chem. Res. 29 (1990) 1822.
[11] D.J. Suh, T.J. Park, S. Ihm, Ind. Eng. Chem. Res. 31 (1992) 1849.
[12] A.M Stratz, in: J.R. Kosak (Ed.), Catalysis of Organic Reactions, Marcel Dekker, New York, 1984, p. 335 and references therein.
[13] G. Neri, M.G. Musolino, L. Bonaccorsi, A. Donato, L. Mercadante, S. Galvagno, Ind. Eng. Chem. Res. 36 (1997) 3619.
[14] M.G. Musolino, C. Milone, G. Neri, L. Bonaccorsi, R. Pietropaolo, S. Galvagno, Stud. Surf. Sci. Catal. 108 (1997) 239.
[15] G. Neri, M.G. Musolino, C. Milone, S. Galvagno, Ind. Eng. Chem. Res. 34 (1995) 2226.
[16] G. Neri, M.G. Musolino, C. Milone, A.M. Visco, A. Di Mario, J. Mol. Catal. A 95 (1995) 235.
[17] G. Neri, M.G. Musolino, E. Rotondo, S. Galvagno, J. Mol. Catal. A 111 (1996) 257.
[18] G. Neri, M.G. Musolino, C. Milone, D. Pietropaolo, S. Galvagno, Appl. Catal. A 208 (2001) 307.
[19] M. Boudart, G. Djéga-Mariadassou, in: Kinetics of Heterogeneous Catalytic Reactions, Princeton University Press, Princeton, NJ, 1984, p. 189.
[20] G. La Manna, G. Barone, Zs. Varga, D. Duca, J. Mol. Struct. (Theochem) 548 (2001) 173.
[21] G. Barone, D. Duca, J. Mol. Struct. (Theochem) 584 (2002) 209.
[22] G. Barone, D. Duca, J. Catal., in press (2002).
[23] P.J. Hay, W.R. Wadt, J. Chem. Phys. 82 (1985) 270.
[24] M.J. Frisch, G.W. Trucks, H.B. Schlegel, G.E. Scuseria, M.A. Robb, J.R. Cheeseman, V.G. Zakrzewski, J.A. Montgomery, R.E. Stratmann, J.C. Burant, S. Dapprich, J.M. Millam, A.D. Daniels, K.N. Kudin, M.C. Strain, O. Farkas, J. Tomasi, V. Barone, M. Cossi, R. Cammi, B. Mennucci, C. Pomelli, C. Adamo, S. Clifford, J. Ochterski, G.A. Petersson, P.Y. Ayala, Q. Cui, K. Morokuma, D.K. Malick, A.D. Rabuck, K. Raghavachari, J.B. Foresman, J. Cioslowski, J.V. Ortiz, B.B. Stefanov, G. Liu, A. Liashenko, P. Piskorz, I. Komaromi, R. Gomperts, R.L. Martin, D.J. Fox, T. Keith, M.A. Al-Laham, C.Y. Peng, A. Nanayakkara, C. Gonzalez, M. Challacombe, P.M.V. Gill, B.G. Johnson, W. Chen, M.W. Wong, J.L. Andres, M. Head-Gordon, E.S. Replogle, J.A. Pople, Gaussian 98, Revision A.6, Gaussian, Inc., Pittsburgh, PA, 1998.
[25] A. Guinier, G. Fournet, in: Small Angle Scattering of X-rays, Chapman & Hall, London, 1959.
[26] J.I. Steinfeld, J.S. Francisco, W.L. Hase, in: Chemical Kinetics and Dynamics, 2nd Edition, Prentice-Hall, Upper Saddle River, NJ, 1998, p. 124.
[27] J.C Bertolini, J. Massadier, in: D.A. King, D.P. Woodruff (Eds.), The Chemical Physics of Solid Surfaces, Vol. 3B, Elsevier, Amsterdam, 1984, p. 133.
[28] W.H. Press, S.A. Teukolsky, W.T. Vetterling, B.P. Flammery, in: Numerical Recipes, Cambridge University Press, Cambridge, 1992.